PHYSICAL REVIEW A VOLUME 10, NUMBER 2 AUGUST 1974

Photoelectric-effect investigations with linearly polarized 1368-keV photons

B. A. Logan and R. T. Jones
University of Ottawa-Carleton University Nuclear Physics Group, University of Ottawa, Ottawa, Canada

A. Ljubičić
Institute Rudjer Bošković, Zagreb, Yugoslavia

W. R. Dixon and R. S. Storey
National Research Council, Ottawa, Canada

(Received 11 April 1973; revised manuscript received 19 February 1974)

The spatial distribution of photoelectrons ejected from the K shell of gold atoms by linearly polarized 1368-keV photons has been measured for photoelectron emission angles in the range 18°–82°. The experimental results are in good agreement with existing theoretical predictions when the predictions are modified to allow for distortion produced by scattering of the photoelectrons in the photoelectric target.

I. INTRODUCTION

Theoretical predictions of the angular distribution of photoelectrons ejected from the K shell of atoms by linearly polarized photons are available.[1–4] In recent years two groups have worked independently and their results are in good agreement.[3,4] At forward emission angles the photoelectrons are predicted to be emitted predominantly in the plane of polarization of the photons. This tendency is less pronounced as the emission angle increases, and for photon energies above a few hundred keV, a crossover is expected to occur and emission in a plane orthogonal to the polarization plane to be favored. The angle at which crossover occurs is expected to decrease with increase of the photon energy.

There are technical difficulties in obtaining suitable beams of linearly polarized photons and only a few investigations of the spatial distribution of the photoelectrons have been reported.[5–9] In these investigations the linearly polarized photons were obtained from either Compton scattering of ^{60}Co γ rays or by an arrangement involving annihilation radiation. The accuracy of the results was limited owing to such factors as poor energy resolution of the photon beam, poor energy resolution of the detection system, and the low degree of linear polarization of the photon beams. It was also difficult to correct for the large distortions which were produced by multiple scattering of the photoelectrons in the photoelectric target. The results of different experiments have been in conflict and, in all cases, the investigations were limited to photon energies well below 1 MeV.

This paper reports an experimental investigation of the spatial distribution of photoelectrons ejected from the K shell of gold atoms by linearly polarized 1368-keV photons. The nuclear reaction ^{24}Mg$(p, p'\gamma)^{24}$Mg was used to supply an intense, monoenergetic, highly polarized photon beam and it was possible to obtain data of good quality. At this energy it was possible to make a realistic correction of distortions produced by scattering of the photoelectrons in the photoelectric target and a detailed comparison between the experimental results and the theoretical predictions was possible. A preliminary account of this work has been given.[10]

II. EXPERIMENTAL

A. Source of the linearly polarized photons

Intense beams of linearly polarized photons are often produced in $(p, p'\gamma)$ reactions. In the reaction ^{24}Mg$(p, p'\gamma)^{24}$Mg resonances at proton energies of 2.01 and 2.40 MeV, corresponding to compound nuclear states of ^{25}Al with positive parity and spins of $\frac{3}{2}$ and $\frac{5}{2}$, have often been used to produce linearly polarized 1368-keV photon beams suitable for the calibration of γ-ray polarimeters.[11–13] These $E2$ γ rays are produced in the deexcitation of the 2^+ first excited state of ^{24}Mg. Their linear polarization is high because the outgoing inelastically scattered protons are predominantly s wave.[11] With a quantization axis along the incident proton-beam direction only $\pm\frac{1}{2}$ magnetic sublevels of the compound nuclear level of ^{25}Al can be occupied and these levels can only decay, via s-wave proton emission, to the 0 and ± 1 sublevels of the 1368-keV 2^+ state of ^{24}Mg. The angular distribution of the $\Delta m = 0$ $E2$ component is such that no γ rays are emitted at 90° to the axis of quantization. The $\Delta m = \pm 1$ $E2$ transitions emitted at 90° to the quantization axis give radiation completely polarized in the plane of the incident proton and

the emitted γ rays. The $\frac{3}{2}^+$ and $\frac{5}{2}^+$ levels in ^{25}Al can also decay to the 2^+ level of ^{24}Mg via d-wave proton emission and this allows the ± 2 sublevels of the 2^+ state to be occupied. The subsequent $\Delta m = \pm 2$ $E2$ transitions reduce the degree of linear polarization of the γ rays emitted at 90° to the quantization axis.[11]

The angular distribution $W(\theta)$ of $E2$ γ rays emitted in a reaction can be written as

$$W(\theta) = 1 + a_2 P_2(\theta) + a_4 P_4(\theta), \quad (1)$$

where a_2 and a_4 are angular distribution coefficients and $P_2(\theta)$ and $P_4(\theta)$ are Legendre polynomials.

The linear polarization of $E2$ γ rays emitted at 90° to the proton-beam direction is given by[14]

$$P(90°) = \frac{1.5a_2 + 0.625a_4}{1 - 0.5a_2 + 0.375a_4} . \quad (2)$$

In this notation P is expressed in the form $P = (I_1 - I_2)/(I_1 + I_2)$, where I_1 is the intensity of the photons with their electric vector in the plane containing the incident proton, and the emitted photon and I_2 is the intensity of the photons with their electric vector orthogonal to this plane. $P(90°)$ can be estimated from a measurement of $W(\theta)$.

In our experimental arrangement a 3.07-MeV proton beam from the 4-MV Van de Graaff accelerator of the National Research Council of Canada was incident on a magnesium target whose thickness was greater than the range of the protons. This arrangement has the advantage of exciting several compound nuclear resonances simultaneously, and a considerable enhancement of the photon intensity is achieved. A resonance at a proton energy of 2.93 MeV contributes strongly to the yield. The angular distribution of the γ rays was measured and the linear polarization P of the photons emitted at 90° to the proton-beam direction was found to be 0.71 ± 0.03. The details of this measurement have been reported.[16] The number of γ rays emitted per unit time at a mean-emission angle of 90° was measured and compared with the counting rate produced by the 1332-keV photons of a ^{60}Co source of known activity placed at the target position. The counting rate of the γ rays from the magnesium was, for a typical beam current of 100 μA, approximately the same as would be produced by the 1332-keV photons of a

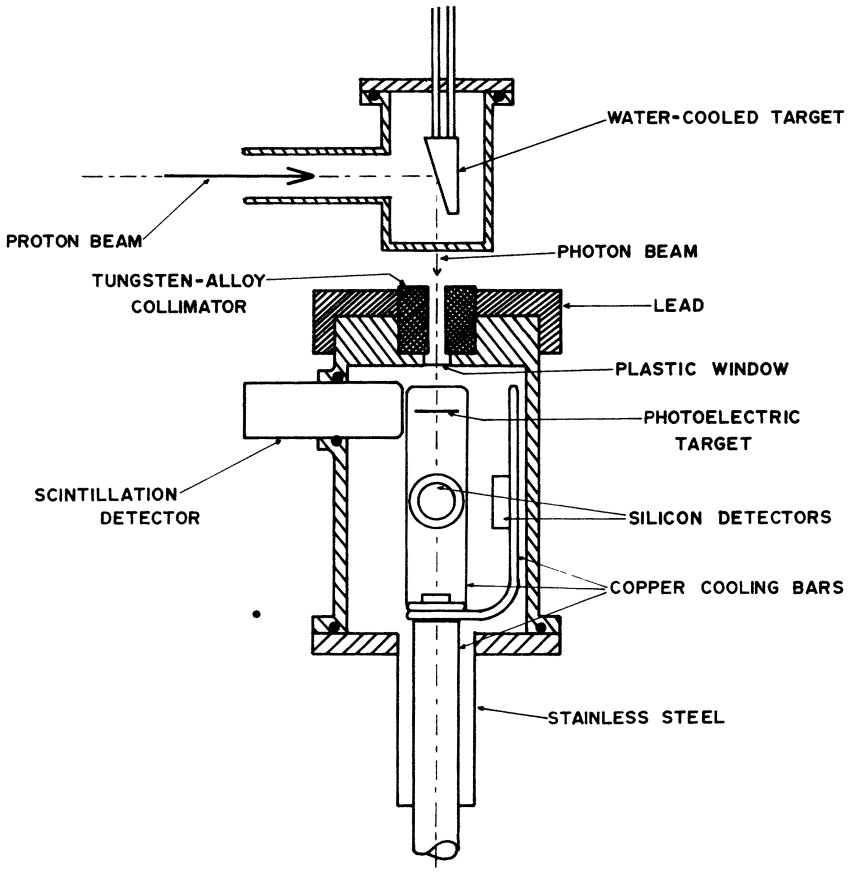

FIG. 1. Diagram of the basic experimental arrangement.

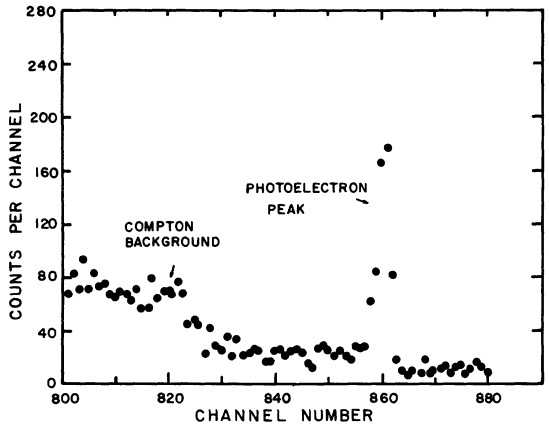

FIG. 2. Gated spectrum obtained in one of the Si(Li) detectors. The spectrum was obtained for $\theta = 45°$ and with a 9.8-mg/cm^2 gold-foil target.

30-mCi ^{60}Co source.

The statistical characteristics of polarized photon beams has been discussed.[15,16] On a statistical basis the quality of a polarized photon beam varies as $(I_1 + I_2)P^2$ and, using this product as a quality criterion, our experimental arrangement was approximately seven times better than an arrangement involving only the 2.40-MeV resonance in the ^{24}Mg$(p, p'\gamma)^{24}$Mg reaction.

B. Measurement of the spatial distribution of the photoelectrons

A diagram of the basic experimental arrangement is shown in Fig. 1. The magnesium-target assembly and the apparatus containing the photoelectric target and detectors have been described previously.[8,13] After being collimated by passing through a $\frac{3}{8}$-in.-diam hole in a $2\frac{5}{8}$-in.-deep tungsten-alloy collimator, the photons emitted vertically downwards from the target assembly entered the evacuated apparatus containing the gold photoelectric target. The gold target was about 6 in. below the magnesium target.

Electrons ejected from the gold target were detected by a pair of cooled 2-cm^2-area Si(Li) detectors mounted on copper bars which extended outside the evacuated apparatus into a liquid-nitrogen container. The Si(Li) detectors were mounted in, and perpendicular to, the plane of polarization of the photons at equal angles with respect to the central geometrical axis. Two pairs of detectors were used: one pair had a depletion depth of 5 mm and the other pair a depletion depth of 3 mm. Both pairs could be moved along the copper bars to allow measurements to be made at different photoelectron emission angles. All the detectors had an energy resolution (full width at half-maximum) of about 15 keV for 1332-keV photons at the high counting rates experienced in the experiments.

Gold K x rays were detected in $(\frac{1}{4} \times 1)$-in-diam NaI(Tl) detectors placed near the gold target. A coincidence was required between a Si(Li) detector and either of the NaI(Tl) detectors and was used to gate the Si(Li) counter spectra which were recorded in multichannel analyzers. The electronic arrangement was conventional. The coincidence resolving times as defined by the time-to-pulse-height converter and timing channel-analyzer combination was about 200 nsec in each case. Spectra from both the Si(Li) detectors were recorded simultaneously and a typical spectrum is shown in Fig. 2. A considerable background due to random events and unsuppressed Compton events was present at low energies but clear photoelectron peaks were obtained and, in this region of the spectrum, random coincidences were negligible.

The ratio $R(\theta)$ of the number of K-shell photoelectrons ejected in the polarization plane to the number emitted in a plane perpendicular to this was measured for various values of the photoelectron emission angle θ. At forward angles the gold target was mounted normal to the incident photon beam. However, at backward angles the target was angled to this direction in order to minimize the energy spread of the emitted photoelectrons and to reduce complications produced by the multiple scattering of the photoelectrons in the target. Two measurements were made at each θ, the second

TABLE I. Measured values of $R(\theta)$, theoretical predictions of $R(\theta)$, and modified theoretical predictions of $R(\theta)$.

Emission angle of the photoelectrons (deg)	Gold target thickness (mg/cm^2)	Uncorrected theoretical value of $R(\theta)$	Modified theoretical value of $R(\theta)$	Measured value of $R(\theta)$
18 ± 5	4.9	2.18	1.64	1.50 ± 0.20
24 ± 6	4.9	1.80	1.56	1.70 ± 0.16
32 ± 9	9.8	1.47	1.37	1.47 ± 0.17
45 ± 5	9.8	1.04	1.10	0.99 ± 0.10
66 ± 7	9.8	0.75	0.93	1.01 ± 0.15
82 ± 9	9.8	0.66	0.88	0.85 ± 0.12

measurement being made with the apparatus containing the photoelectric target and the detectors being rotated by 90°, about a vertical axis, from the orientation of the first measurement. This procedure cancels out false asymmetries which can be produced if the two counting channels have different counting efficiencies. Typical beam currents of 50–150 μA allowed a measurement at a given orientation to be completed in 4–10 h.

A systematic false asymmetry can still be produced if the photon beam is not symmetrically distributed around the symmetry axis of the photoelectric-target detector system. Detailed investigations made with a ^{60}Co source deliberately displaced from the symmetry axis of the system indicated that false asymmetries, which could be produced by such geometrical misalignments, were less than 5% in all cases.

III. RESULTS

The experimental values of $R(\theta)$ are given in Table I. The uncertainties are statistical standard deviations obtained after a subtraction has been made for the background contributions to the photoelectron peaks. As can be seen from Fig. 2 the background subtractions were not very large. The thickness of the gold target, and the angular ranges subtended by the Si(Li) detectors at the center of the gold target, are also given in Table I.

IV. ANALYSIS

A. Theoretical background

The theoretical predictions[3,4] describe the spatial distribution of photoelectrons ejected from the K shell by linearly polarized photons with a parameter $C_{10}(\theta)$. The differential cross section for the K-shell photoelectrons in the case of photons with a linear polarization P is given by

$$\sigma(\theta, \phi) = \sigma(\theta)[1 + C_{10}(\theta) P \cos 2\phi] , \qquad (3)$$

where $\sigma(\theta)$ is the differential cross section for unpolarized photons. Theoretical predictions of $C_{10}(\theta)$ are available for atoms with atomic numbers from 1 to 100 and for photon energies ranging from 1 keV to 100 MeV.[4] The theoretical $R(\theta)$ distribution can be obtained from these values and is shown in Fig. 3 along with the measured $R(\theta)$ values. Although the experimental results agree with the general trend of the theoretical predictions in that they show photoelectrons emitted at forward angles as being predominantly in the plane of polarization and in that they support the existence of a crossover effect, they do differ significantly from them. For example, the magnitudes of the experimental $R(\theta)$ values do not range as

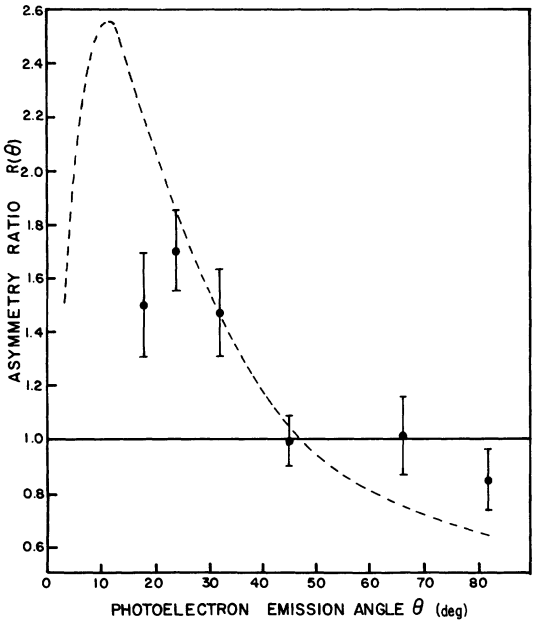

FIG. 3. Theoretical distribution $R(\theta)$ and the measured values of $R(\theta)$.

widely as the theoretical predictions and the crossover seems to occur at a larger emission angle than predicted. However, two effects have not been allowed for. The detectors subtend a range of θ and ϕ values and an averaging of the theoretical predictions has to be made. In addition, although it was possible to use foil thickness which allowed the distortions produced by plural and multiple scattering of the photoelectrons in the gold target to be less than in previous work, it is still necessary to correct for distortions if a detailed comparison between theory and experiment

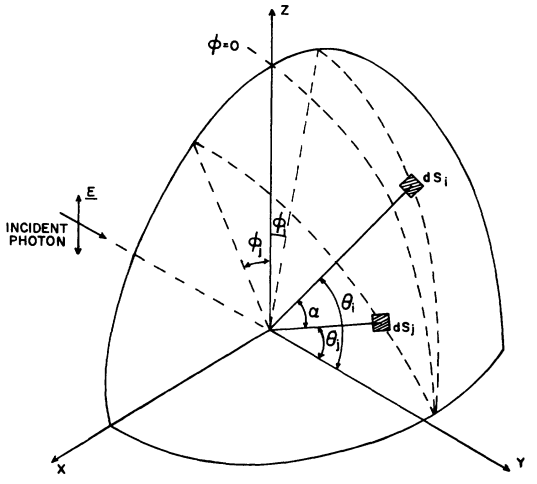

FIG. 4. Diagram of the geometry of the system.

is to be realized. These corrections are discussed in Sec. IV B.

B. Corrections to the theoretical predictions

In principle, corrections could be made to the experimental data to allow a more realistic comparison with the theoretical predictions. In practice it is more convenient to modify the theoretical predictions. This is done by averaging the predictions over the experimental angular range of the emitted photoelectrons and by estimating how the theoretical angular distribution would be modified by the scattering experienced by the photoelectrons in the photoelectric target. The modified theoretical distribution can then be compared with the experimental results. The calculations involving the averaging over angular ranges, and correcting for scattering distortions, were made with the assistance of an IBM 360/65 computer.

The geometry of the system is shown in Fig. 4. The linearly polarized photon beam is incident along the y axis and the plane of polarization is in the yz plane. The origin of the coordinate system is at the center of the photoelectric target. As photoelectrons produced at different depths inside the target will undergo varying amounts of scattering, the first step in the analysis was to divide the target into a number of 1-mg/cm^2 sections. The scattering distortions experienced by photoelectrons produced at the center of each section was calculated separately, and the final total modified distribution was estimated by summing the contributions from each section.

The number of photoelectrons produced per unit time inside a section of the target and initially directed towards a surface element of area dS_j on the geometrical sphere of radius R is given by

$$n_j = K\sigma(\theta_j\phi_j)dS_j \ . \tag{4}$$

The constant K includes such factors as the incident photon flux, the number of K-shell photoelectrons in the target section, and R, the radius of the geometrical sphere of which dS_j is a surface element.

The number of photoelectrons which are scattered inside the target through an angle α into a solid angle $d\Omega_j$ is given by

$$N_{ji} = n_j W_{ij}(\alpha)\, d\Omega_i \ , \tag{5}$$

where $d\Omega_i$ is part of the solid angle subtended by a detector and $W_{ij}(\alpha)$ is the scattering distribution which measures the probability of this scattering occurring. $W_{ij}(\alpha)$ depends on such parameters as the electron energy, the atomic number of the scattering medium, and on the effective target thickness presented to a photoelectron. This latter dependence leads to complications in our case.

As has already been noted, the effective thickness presented to a photoelectron will depend on where it is produced but, in addition to this, it will also depend on θ_j. The combination of these two factors leads to wide variations in the effective target thickness presented to different photoelectrons and different situations must be considered. If the effective target thickness is small, plural-scattering theories are applicable while at larger thicknesses more scatterings will take place inside the target and multiple-scattering theories are more suitable.

The effective target thickness was calculated for each photoelectron path analyzed. The expected number of scatterings it would experience was calculated from the well-known formula given by Molière.[17] If the expected number of scatterings was less than 20, $W_{ij}(\alpha)$ was taken from the plural-scattering calculations of Keil, Zeitler, and Zinn.[18] If the number of scatterings was more than 20 it was assumed that $W_{ij}(\alpha)$ could be taken from the theory of Molière.[17]

The number of photoelectrons N_{js}, which are emitted at (θ_j, ϕ_j) and which are scattered towards a detector of area S, can be found by summing relation (5) over the index i,

$$N_{js} = \sum_i n_j W_{ij}(\alpha) d\Omega_i \ . \tag{6}$$

The analysis outlined above assumes that the photoelectrons were produced along the central geometrical axis of the target detector system.

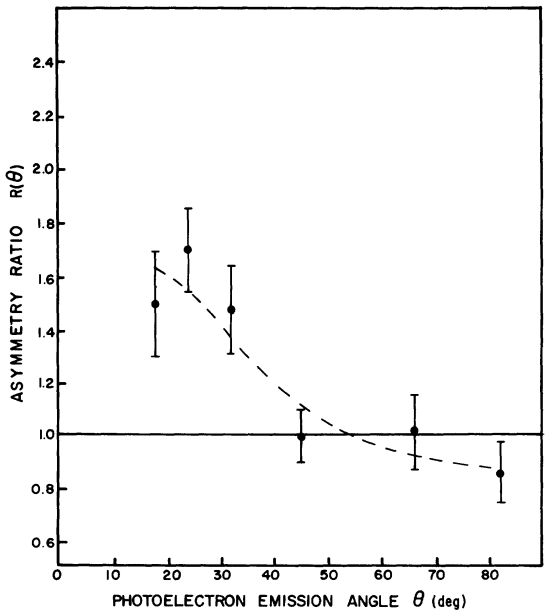

FIG. 5. Hand-drawn line through the modified $R(\theta)$ values and the measured values of $R(\theta)$.

This is a reasonable approximation if the target area is small compared with the area of the detector. However, this is not the situation in our experimental arrangement. Our situation could be simulated by making calculations for a variety of positions of the photoelectric target but this could be very time consuming. The most important consequence of the finite target area is to increase the ranges of the photoelectron emission angles. In order to make some allowance for this a calculation was made for a point source but it was assumed that the areas of the detectors were greater than their geometrical areas. The ranges of θ and ϕ were taken to correspond to the angular ranges subtended by the diagonal of a rectangular area being of such a length that its extremities represented the angular ranges of the emitted photoelectrons when an allowance is made for both the size of the photoelectric target and the area of the Si(Li) detector.

By summing relation (6) over the index j it is possible to obtain the number of photoelectrons emitted from a section inside the target in all possible directions which can give emission onto the surface of a detector. Finally, when a summation is made to allow for the contributions from the different 1-mg/cm^2 sections inside the target it is possible to calculate the number of photoelectrons emitted onto the surface of each detector.

The range of validity of the Molière theory is expected to be limited to situations where the maximum value of the mean scattering angle $\bar{\alpha}$ is less than 20°. In our case photoelectrons are emitted in all directions and some of them will have large path lengths in the target; the value of $\bar{\alpha}$ for these paths will be above 20°. Nevertheless, in the analysis a requirement was made that the maximum value of $\bar{\alpha}$ be less than 22°. Although this value is near the upper limit of the validity of the Molière theory the choice was not arbitrary. Calculations assuming different values for the maximum value allowed for α gave converging results as the maximum value of $\bar{\alpha}$ was increased. In particular, the final results for maximum limits on $\bar{\alpha}$ ranging from 16° to 22°, were in agreement within 2%.

Although the estimates of the distortions produced by the scattering processes involve approximations, the intense photon beam available in our experimental arrangement allowed relatively thin photoelectric targets to be used and the distortions were not too excessive. For example, the mean value $\bar{\alpha}$ for 1300-keV electrons incident normal to a 7-mg/cm^2 gold foil is only about 14°. Consequently, any uncertainties in the corrections have a reduced effect on the uncertainties of the final modified theoretical predictions.

The modified $R(\theta)$ values are given in Table I. Although the modified $R(\theta)$ values were only calculated for the experimental configurations a hand-drawn line through the values is shown in Fig. 5. The effects of the averaging procedure, and of the scattering distortions, are to reduce the magnitude of the $R(\theta)$ values and to move the crossover angle to a larger value of θ.

V. CONCLUSIONS

A new experimental technique has been developed for investigating the spatial distribution of K-shell photoelectrons ejected by linearly polarized photons. It has allowed new data to be obtained at a photon energy of 1368 keV, a much higher energy than any energies investigated previously. It was also possible to make a realistic estimate of the distortions produced by scattering of the photoelectrons in the photoelectric target. When existing theoretical predictions are modified to make allowances for the distortions produced by the scattering processes good agreement is obtained with our experimental results. It is concluded that our experimental results are in support of the validity of the theoretical predictions.

ACKNOWLEDGMENTS

We thank Dr. J. M. Robson and Dr. R. L. Clarke for encouragement in the earlier stages of this work and Dr. R. H. Pratt and Dr. S. Hultberg for private communications. Also thanks are due to Dr. Hultberg for theoretical predictions relevant to the experimental conditions. The authors are grateful to D. C. Elliott, G. D. Smith, and J. D. Stinson for assistance during the experiments. One of us (B. A. L.) also wishes to thank the National Research Council and the Atomic Energy Control Board of Canada for financial support.

[1]F. Sauter, Ann. Phys. 11, 454 (1931).
[2]F. Sauter and H. O. Wüster, Z. Phys. 141, 83 (1955).
[3]R. H. Pratt, R. D. Levee, R. L. Pexton, and W. Aron, Phys. Rev. 134, A898 (1964); 134, A916 (1964).
[4]S. Hultberg, B. Nagel, and P. Olsson, Ark. Fys. 38, 1 (1968).
[5]F. L. Hereford and J. L. Keuper, Phys. Rev. 90, 1043 (1953).
[6]W. H. McMaster and F. L. Hereford, Phys. Rev. 95, 723 (1954).
[7]D. Brini, L. Pelli, O. Rimondi, and P. Veronesi, Nuovo Cimento 6, 98 (1957).

[8]B. A. Logan, Nucl. Instrum. Methods 82, 149 (1970).
[9]B. A. Logan, J. Phys. A 4, 346 (1971).
[10]R. T. Jones, B. A. Logan, A. Ljubičić, W. R. Dixon, and R. S. Storey, Bull. Am. Phys. Soc. 18, 142 (1973).
[11]A. E. Litherland and H. E. Gove, Can. J. Phys. 39, 471 (1961).
[12]G. T. Ewan, G. I. Anderson, G. A. Bartholomew, and A. E. Litherland, Phys. Lett. B 29, 352 (1969).
[13]A. Ljubičić and B. A. Logan, Nucl. Instrum. Methods 99, 269 (1972).
[14]L. W. Fagg and S. S. Hanna, Rev. Mod. Phys. 31, 711 (1959).
[15]B. A. Logan, R. T. Jones, and A. Ljubičić, Nucl. Instrum. Methods 108, 603 (1973).
[16]W. R. Dixon, R. S. Storey, A. Ljubičić, R. T. Jones, and B. A. Logan, Nucl. Instrum. Methods 113, 149 (1973).
[17]G. Molière, Z. Naturforsch. A3, 78 (1948).
[18]E. Keil, E. Zeitler, and W. Zinn, Z. Naturforsch. A15, 1031 (1960).